Accepted Manuscript

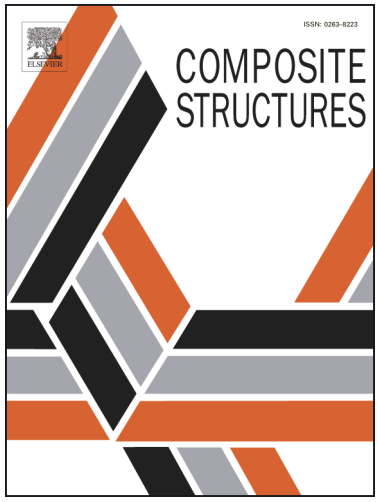

Effect of beam orientation on the static behaviour of phenolic core sandwich composites with different shear span-to-depth ratios

Wahid Ferdous, Allan Manalo, Thiru Aravinthan

PII: S0263-8223(16)32388-1
DOI: http://dx.doi.org/10.1016/j.compstruct.2017.02.061
Reference: COST 8282

To appear in: *Composite Structures*

Received Date: 2 November 2016
Revised Date: 4 January 2017
Accepted Date: 10 February 2017

Please cite this article as: Ferdous, W., Manalo, A., Aravinthan, T., Effect of beam orientation on the static behaviour of phenolic core sandwich composites with different shear span-to-depth ratios, *Composite Structures* (2017), doi: http://dx.doi.org/10.1016/j.compstruct.2017.02.061

This is a PDF file of an unedited manuscript that has been accepted for publication. As a service to our customers we are providing this early version of the manuscript. The manuscript will undergo copyediting, typesetting, and review of the resulting proof before it is published in its final form. Please note that during the production process errors may be discovered which could affect the content, and all legal disclaimers that apply to the journal pertain.

ACCEPTED MANUSCRIPT

Effect of beam orientation on the static behaviour of phenolic core sandwich composites with different shear span-to-depth ratios

Wahid Ferdous, Allan Manalo* and Thiru Aravinthan

Centre for Future Materials (CFM), School of Civil Engineering and Surveying, Faculty of Health, Engineering and Sciences, University of Southern Queensland, Toowoomba, QLD 4350, Australia

Email: md.ferdous@usq.edu.au; allan.manalo@usq.edu.au; thiru.aravinthan@usq.edu.au;

Abstract

This study thoroughly investigated the flexural behaviour of phenolic cored sandwich beams with glass fibre composite skins in the horizontal and vertical positions. The beams have a shear span-to-depth ratio (a/d) varying between 0.5 and 12, and tested under 4-point static bending. Their failure load are then predicted theoretically. The results showed that changing the beam orientation from horizontal to vertical changes the failure mode from brittle to progressive. The sandwich beam's high bending stiffness can be efficiently utilised by placing them vertically. The a/d ratio played a major role on the load capacity and failure mode. In both orientations, the load capacity decreased with the increased of a/d. The beam failed in shear, a combined shear and bending, and bending for $a/d \leq 2$, $2 < a/d < 6$, and $a/d \geq 6$, respectively. These failure mechanisms can be correlated to the shear-to-bending stress ratio while the failure load can be reasonably predicted using the available theoretical models. The two-way analysis of variance showed that the beam orientation is a more influential parameter than the a/d ratio. From this study, the horizontal beams are preferable for flexural dominated structures while the vertical beams are desirable for shear dominated structures.

Keywords

Sandwich beam; Static behaviour; Beam orientation; Shear span-to-depth ratio; Theoretical model.

*Corresponding author, tel. +61 7 4631 2547; fax. +61 7 4631 2110; E-mail addresses: allan.manalo@usq.edu.au (Allan Manalo)

ACCEPTED MANUSCRIPT

1. Introduction

The applications of fibre composite sandwich systems are rapidly increasing in civil infrastructure and construction due to their excellent durability, design flexibility, cost effectiveness, and high strength-to-weight and stiffness-to-weight ratios [1]. In these applications, composite sandwich panels are oriented either in the horizontal or vertical directions to effectively resist the design loading. In particular, sandwich panels in horizontal orientation are widely used for structural roofs [2], floors [3], walls [4] and bridge decks [2]. In this orientation, the strong and stiff fibre composite skins are located at the top and bottom surfaces of the panels. On the other hand, the panels are used in the vertical orientation for bridge girders [3], railway sleepers [5, 6], or similar beam applications wherein the fibre composite skins are located at both sides of the core material.

Several studies have been conducted to investigate the behaviour of sandwich panels at horizontal orientation [7-13] while very limited studies have been reported on the behaviour at vertical position. Manalo et al. [14] are probably the only researchers who evaluated the behaviour of 20 mm × 50 mm sandwich beams in both horizontal and vertical orientations. The results of their experimental investigation showed that the sandwich beams in the vertical position failed at a higher load with less deflection compared to beams in the horizontal position. Similarly, the beams in the vertical orientation failed progressively while the beams in the horizontal orientation exhibited a brittle failure. Their study however was limited to sandwich beams with a particular shear span resulting to beams with different shear-span ratios making the direct comparison of their behavior inadequate. Many researchers [15-17] indicated that shear span-to-depth ratio has a strong influence on the failure behaviour and structural performance of the sandwich beams. Manalo [18] investigated the behaviour of phenolic-core sandwich beams in horizontal orientation with different shear span-to-depth ratios. His study found that with increase of shear span-to-depth

ACCEPTED MANUSCRIPT

ratio, the failure load of the sandwich beam decreases due to the increase of deflection. Recently, Mathieson and Fam [19] studied the bending and failure mechanism of sandwich beams with low-density polyurethane core and glass fiber-reinforced polymer skins in vertical orientation with varying shear span-to-depth ratios in the application of walls and supporting beams. They observed the increase of shear span-to-depth ratio can significantly reduce the moment capacity of the sandwich panel due to the occurrence of the skin wrinkling in compression.

Clearly, there are significant variations in the behaviour of sandwich beams due to the change of orientation and shear span-to-depth ratio. However, the reported studies are limited to the investigation of sandwich beams' behaviour either in the horizontal or vertical orientation making a comparison study necessary and significant. This study investigated the effect of beam orientation on the static behaviour of fibre composite sandwich structure made up of phenolic core and glass fibre composite skins. A total of 30 different specimens with 20 mm × 20 mm, 20 mm × 40 mm and 20 mm × 80 mm sectional dimensions were tested under static bending in horizontal and vertical orientations at different shear span-to-depth (a/d) ratios. The failure behaviour, strength and stiffness properties of the sandwich beams were evaluated. Prediction equations for the failure load of the sandwich beams in different orientations and a/d ratios were also presented and compared with the experimental results. The outcomes of this study provided an indication on how to effectively utilize the composite sandwich beams in carrying loads required in different civil engineering applications.

2. Materials and Methods

2.1. Materials

The structural composite sandwich beams tested in this study consisted of glass fibre reinforced polymer (GFRP) composite layers (skins) bonded to a phenolic core. The fibres of each skin were laid up in 0^0 (4 layers), 90^0 (2 layers) and $\pm 45^0$ (2 layers in each) along the

ACCEPTED MANUSCRIPT

longitudinal direction of the sandwich beam to provide strength and stiffness in all directions. Each skin was 1.8 mm thick with a fibre volume ratio of 45%. The phenolic core material came from natural plant (non-food) products derived from vegetable oils and plant extracts and was chemically bonded with the polymer resin. The density of sandwich panel is approximately 990 kg/m^3 which is comparable to the hardwood red gum timber [20]. The properties of the GFRP skins and phenolic core were determined by the second author and are provided in Table 1.

Table 1: Properties of GFRP skin and phenolic core materials

Test	Properties	GFRP skin		Phenolic core
		Longitudinal	Transverse	
Flexure	Elastic modulus (GPa)	14.28	3.66	1.33
	Peak stress (MPa)	450.39	135.05	14.32
	Strain at peak (%)	2.29	5.26	1.22
Tensile	Elastic modulus (GPa)	15.38	12.63	1.03
	Peak stress (MPa)	291.20	216.27	5.97
	Strain at peak (%)	1.61	2.37	0.61
	Poisson's ratio	0.25	0.13	-
Compressive	Elastic modulus (GPa)	16.10	9.95	1.33
	Peak stress (MPa)	238.04	124.23	21.35
	Strain at peak (%)	1.24	1.25	4.04
	Poisson's ratio	-	-	0.29
Shear	Shear modulus (GPa)	2.47	2.17	0.53
	Peak stress (MPa)	23.19	21.81	4.25
	Strain at peak (%)	3.08	2.38	0.81

ACCEPTED MANUSCRIPT

2.2. Specimen details and test setup

The bending test for sandwich beams was conducted in accordance with ASTM C393 [21]. In the horizontal position, the skins were located at top and bottom while the skins were at both side of phenolic core in vertical position. The specimens were prepared by cutting the panels into the required dimensions using a water jet cutter. The load was applied through a spreader beam with a loading rate of 3 mm/min using the MTS 100 kN testing machine. Three replicates were tested for each specimen type until the ultimate failure. Figures 1(a) and 1(b) illustrated the horizontal and vertical positions of the beam section, respectively with the necessary dimensions while Figure 1(c) shows the typical test setup.

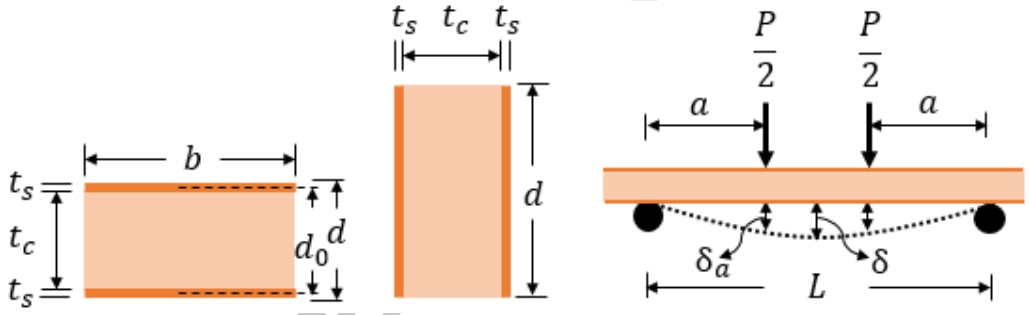

(a) horizontal orientation (b) vertical orientation (c) test setup

Fig. 1: Sectional dimension, orientation and test setup

In Figure 1, the $t_s, t_c, b,$ and d refer to the thickness of skin, thickness of core, beam width and beam depth, respectively. The other parameters $P, a,$ and L represent the applied load, shear span and span of the tested beam, respectively. In this study, t_s and core t_c were same for all 30 specimens. Therefore, the change of beam dimension indicates either the change of width (b) or depth (d). Depending on the test set-up, beam dimension and orientation, the a/d ratios were varying between 0.5 and 12. The variation of a/d ratio was ensured by changing the beam orientation and shear span while maintaining the span of the

ACCEPTED MANUSCRIPT

beams. The details of the 30 different types of sandwich beam specimens are summarised in Table 2.

Table 2: Details of the specimen

Specimen ID	L (mm)	a (mm)	d (mm)	b (mm)	a/d	Beam orientation	Failure loads (N)			Failure mode
							Expt.	Theo.	%Diff.	
$A_{40}D_{20}W_{20}H$	480	40	20	20	2	Horizontal	3375	2954	-12	CS
$A_{40}D_{20}W_{20}V$	480	40	20	20	2	Vertical	2237	2905	30	SS
$A_{40}D_{20}W_{40}H$	480	40	20	40	2	Horizontal	6582	5907	-10	CS
$A_{40}D_{40}W_{20}V$	480	40	40	20	1	Vertical	5924	5811	-2	SS
$A_{40}D_{20}W_{80}H$	480	40	20	80	2	Horizontal	12262	11814	-4	CS
$A_{40}D_{80}W_{20}V$	480	40	80	20	0.5	Vertical	12903	7147	-45	I
$A_{80}D_{20}W_{20}H$	480	80	20	20	4	Horizontal	2367	1672	-29	CS+D
$A_{80}D_{20}W_{20}V$	480	80	20	20	4	Vertical	1309	1135	-13	SS+SC
$A_{80}D_{20}W_{40}H$	480	80	20	40	4	Horizontal	4525	3344	-26	CS+D
$A_{80}D_{40}W_{20}V$	480	80	40	20	2	Vertical	4417	5811	32	SS
$A_{80}D_{20}W_{80}H$	480	80	20	80	4	Horizontal	9014	6687	-26	CS+D
$A_{80}D_{80}W_{20}V$	480	80	80	20	1	Vertical	9572	7147	-25	I
$A_{120}D_{20}W_{20}H$	480	120	20	20	6	Horizontal	2075	2568	24	SC+D
$A_{120}D_{20}W_{20}V$	480	120	20	20	6	Vertical	1087	1242	14	SC+B
$A_{120}D_{20}W_{40}H$	480	120	20	40	6	Horizontal	4072	5136	26	SC+D
$A_{120}D_{40}W_{20}V$	480	120	40	20	3	Vertical	3354	2679	-20	SS+SC
$A_{120}D_{20}W_{80}H$	480	120	20	80	6	Horizontal	8309	10272	24	SC+D
$A_{120}D_{80}W_{20}V$	480	120	80	20	1.5	Vertical	8494	7147	-16	I
$A_{160}D_{20}W_{20}H$	480	160	20	20	8	Horizontal	1571	1926	23	SC+D
$A_{160}D_{20}W_{20}V$	480	160	20	20	8	Vertical	815	932	14	SC+B
$A_{160}D_{20}W_{40}H$	480	160	20	40	8	Horizontal	3241	3852	19	SC+D
$A_{160}D_{40}W_{20}V$	480	160	40	20	4	Vertical	2524	2271	-10	SS+SC
$A_{160}D_{20}W_{80}H$	480	160	20	80	8	Horizontal	6533	7704	18	SC+D
$A_{160}D_{80}W_{20}V$	480	160	80	20	2	Vertical	7228	7147	-1	I
$A_{240}D_{20}W_{20}H$	480	240	20	20	12	Horizontal	1072	1284	20	SC+D
$A_{240}D_{20}W_{20}V$	480	240	20	20	12	Vertical	545	621	14	SC+B
$A_{240}D_{20}W_{40}H$	480	240	20	40	12	Horizontal	2222	2568	16	SC+D
$A_{240}D_{40}W_{20}V$	480	240	40	20	6	Vertical	1950	2485	27	SC+B
$A_{240}D_{20}W_{80}H$	480	240	20	80	12	Horizontal	4594	5136	12	SC+D
$A_{240}D_{80}W_{20}V$	480	240	80	20	3	Vertical	5393	5358	-1	SS+SC

ACCEPTED MANUSCRIPT

CS: Core shear	SS: Skin shear
CS+D: Core shear and debonding	I: Indentation
SC+D: Skin compression and debonding	SS+SC: Skin shear and skin compression
	SC+B: Skin compression and buckling

3. Results and Discussion

3.1. Failure mode

The typical failure modes of the sandwich beams made of GFRP skins and phenolic core are provided in Figure 2(a) to 2(h). These failure modes can be classified into four broad categories, i.e. (a) shear failure, (b) combined shear and bending failure, (c) bending failure, and (d) indentation failure. The following presents a brief description of the different failure modes:

- *Shear failure:* Shear failure of the sandwich beam is illustrated by the diagonal cracks observed either in the phenolic core or GFRP skins between the loading point and the support. This type of failure occurred when the shear stress exceeded the shear strength either of the core or the skins. The specimens (e.g., $A_{40}D_{20}W_{20}H$, $A_{40}D_{20}W_{40}H$ and $A_{40}D_{20}W_{80}H$) at horizontal orientation (Fig. 2(a)) failed instantly due to core shear (CS) at the point of load application. On the other hand, the failure of the specimens at vertical orientation (Fig. 2(b)) was governed by skin shear (SS). With the increase of load, a number of diagonal cracks appeared progressively at the skins in the shear span which resulted in gradual decrease of stiffness (e.g., $A_{40}D_{20}W_{20}V$, $A_{40}D_{40}W_{20}V$ and $A_{80}D_{40}W_{20}V$).
- *Combined shear and bending failure:* This kind of failure occurred when the sandwich beam specimens were subjected to significant amount of combined shear and bending stress. In horizontal orientation (Fig. 2(c)), the specimens failed in core shear followed by the propagation of cracks towards the edge of the specimen and debonding (CS + D) between skin and core (e.g., $A_{80}D_{20}W_{20}H$, $A_{80}D_{20}W_{40}H$ and

ACCEPTED MANUSCRIPT

$A_{80}D_{20}W_{80}H$). In vertical orientation (Fig. 2(d)), the failure was initiated by core cracking and then a number of small shear cracks progressively appeared before the crushing of the skin at top due to compression (SS + SC) followed by the skin splintering at bottom due to tension. The beam lost its load carrying capacity once it was failed by skin compression (e.g., $A_{80}D_{20}W_{20}V$, $A_{120}D_{40}W_{20}V$, $A_{160}D_{40}W_{20}V$ and $A_{240}D_{80}W_{20}V$).

- *Bending failure:* In horizontal orientation (Fig. 2(e)), bending failure was observed between the loading points and initiated by the compressive failure of the top skin followed by debonding (SC + D) between the skin and the core. The core compression simultaneously occurred with debonding which started from the loading point (e.g., $A_{120}D_{20}W_{20}H$, $A_{120}D_{20}W_{40}H$, $A_{120}D_{20}W_{80}H$, $A_{160}D_{20}W_{20}H$, $A_{160}D_{20}W_{40}H$, $A_{160}D_{20}W_{80}H$, $A_{240}D_{20}W_{20}H$, $A_{240}D_{20}W_{40}H$ and $A_{240}D_{20}W_{80}H$). In vertical orientation (Fig. 2(f)), the bending failure was initiated by core cracking at the bottom surface under the loading point. The load continued to increase until failure of skins due to the combined effect of skin compression and buckling (SC + B) followed by the skin tension (e.g., $A_{120}D_{20}W_{20}V$, $A_{160}D_{20}W_{20}V$, $A_{240}D_{20}W_{20}V$ and $A_{240}D_{40}W_{20}V$).
- *Indentation failure:* Indentation occurred due to the high local stress of the sandwich beams in vertical orientation which under four-point bending behaves a specimen under compression and local load transfers from the indenter to the beam, particularly at short shear spans (e.g., $A_{40}D_{80}W_{20}V$, $A_{80}D_{80}W_{20}V$, $A_{120}D_{80}W_{20}V$ and $A_{160}D_{80}W_{20}V$). The load was transferred to supports through compressive stresses that created the local compression at load points and the initiation of the indentation (I) process started (Fig. 2g). However, the same beam (20 mm × 80 mm) with a shear span of 240 mm (e.g., $A_{240}D_{80}W_{20}V$) failed due to bending (Fig. 2h).

ACCEPTED MANUSCRIPT

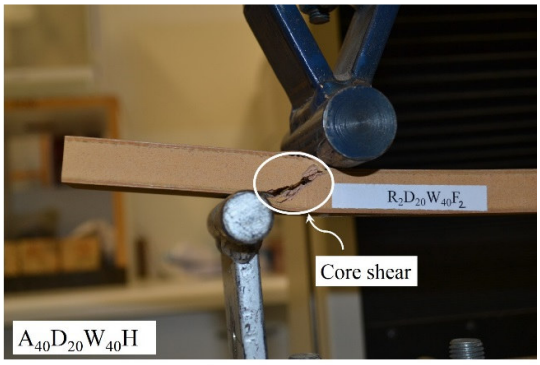

(a) core shear (CS)

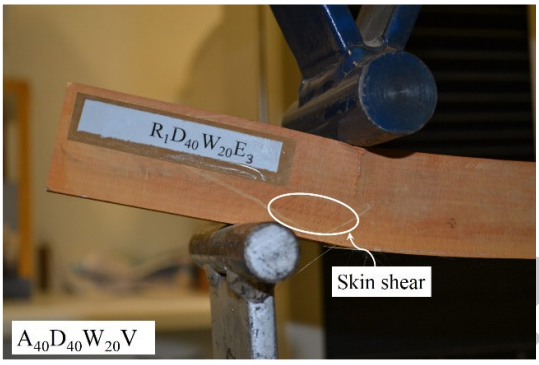

(b) skin shear (SS)

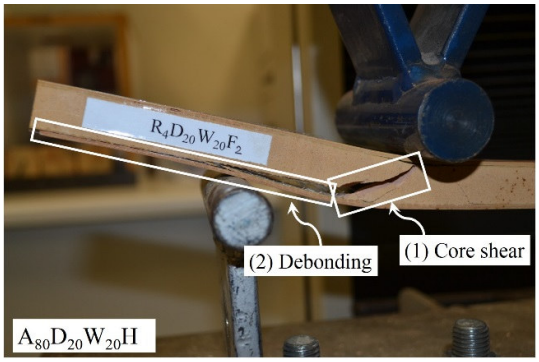

(c) core shear and debonding (CS + D)

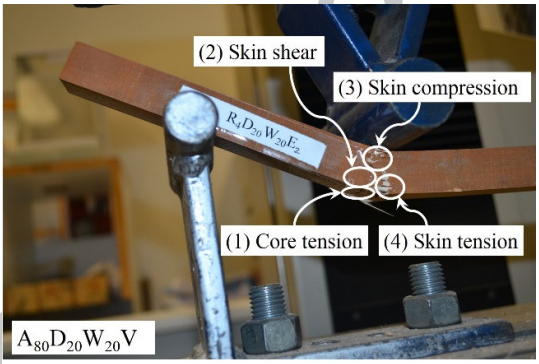

(d) skin shear and skin compression (SS + SC)

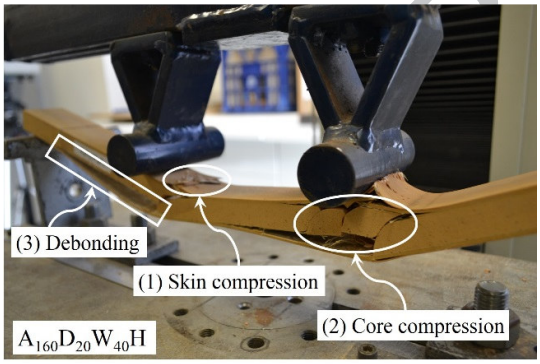

(e) skin compression and debonding (SC + D)

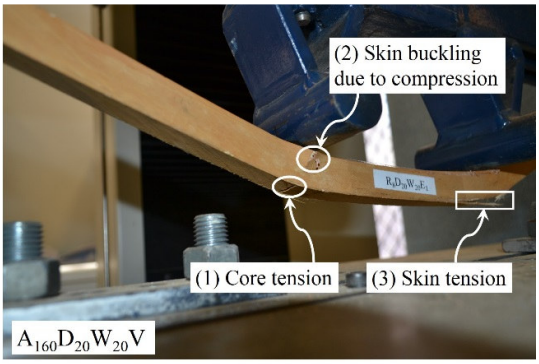

(f) skin compression and buckling (SC + B)

ACCEPTED MANUSCRIPT

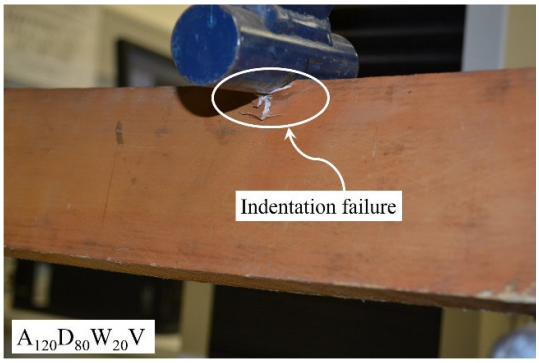

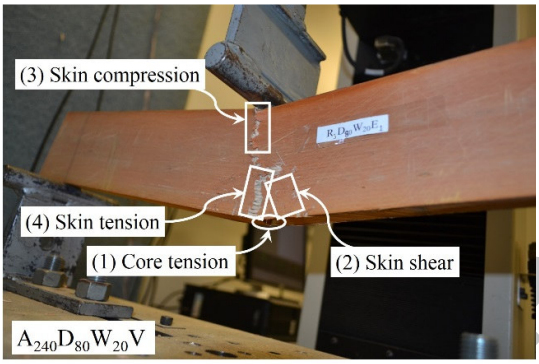

(g) indentation (I), shear span up to 160 mm (h) different failure at shear span of 240 mm

Fig. 2: Failure modes of the composite sandwich beam

3.2. Load-displacement behaviour

The applied load and corresponding displacement at the loading point (δ_a) were recorded using a data logger. From the measured δ_a, the mid-span displacement (δ) was calculated following the relation given in Eq. (1). The load and mid-span displacement behaviour of the sandwich beams in the horizontal orientation are presented in Figures 3(a), 3(c) and 3(e) while the beams in the vertical orientation are shown in Figures 3(b), 3(d) and 3(f).

$$\delta = \frac{\delta_a}{4}\left(\frac{3L^2-4a^2}{3La-4a^2}\right) \quad (1)$$

At 40 mm shear span, a significant drop in load was observed in the horizontal beams before the final failure as shown in Figures 3(a), 3(c) and 3(e). The first drop of the load was observed due to the core shear at one end between the loading point and the support. However, the load increase again with almost same stiffness prior to the first core shear failure. At almost the same load before the first load drop, the second and ultimate drop of the load was observed due to the core shear failure at the other end of the beam. On the other hand, the specimens in vertical orientation with 40 mm shear span showed different behaviour as shown in Figures 3(b), 3(d) and 3(f). A linear elastic behaviour was observed at the early application of the load. Thereafter, a slight drop of load was observed but the beam specimens continued to carry the load due to the effect of core shear compression. A

ACCEPTED MANUSCRIPT

nonlinear load deflection behaviour was further observed prior to failure due to the progressive developments of either shear cracks in the skin or indentation (Figures 2b and 2g).

At 80 mm and 120 mm shear spans with horizontal orientation (Figs. 3a, 3c and 3e), the initiation of debonding between top skin and core occurred at the loading points in several stages that causes staggering pattern in the load-displacement curve. However, this behaviour was gradually transformed into the single stage failure mode when shear span was 160 mm and 240 mm (Figs. 3a, 3c and 3e). On the other side, at 80 mm, 120 mm, 160 mm and 240 mm shear spans with vertical orientation (Figs. 3b, 3d and 3f), the load-displacement behaviour was linear up to a certain point and then it showed a non-linear behaviour. This nonlinearity was initiated by the tensile cracking of the phenolic core followed by compressive failure of the skin. However, the failure of the core in tension does not indicate the ultimate failure of the beam as the vertical skins continue to carry the loads. One obvious difference between horizontal and vertical orientation is that the load dropped suddenly at horizontal orientation whereas the load gradually decreased for vertical beams.

For 20 mm × 20 mm beam section (Fig. 3a and 3b), the higher displacement was noticed in vertical than horizontal orientation at a certain magnitude of loads. However, the horizontal orientation provided the greater displacement for 20 mm × 40 mm (Fig. 3c and 3d) and 20 mm × 80 mm (Fig. 3e and 3f) beam. Moreover, for the same orientation and dimension, it is observed that the increase of shear span decreases the load carrying capacity of the specimens. In addition, at the same level of loads, the specimens with greater shear span deflected more than the specimens with smaller shear span.

ACCEPTED MANUSCRIPT

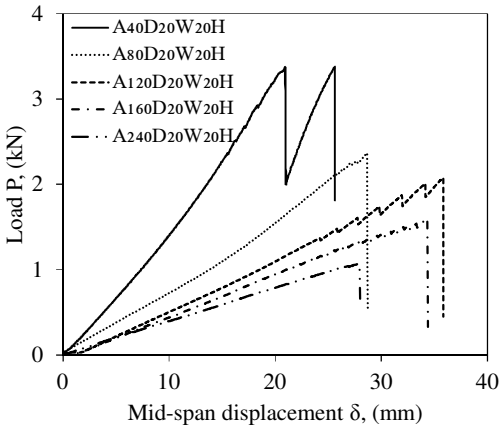

(a) 20 × 20 mm at horizontal orientation

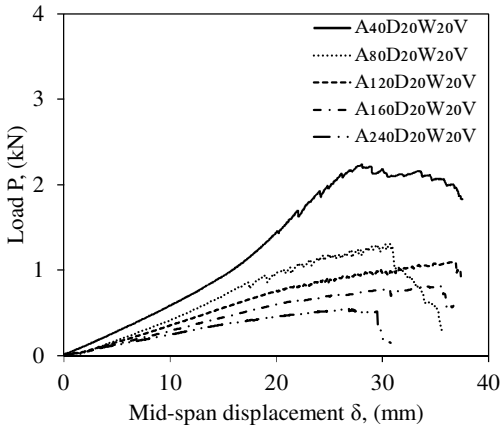

(b) 20 × 20 mm at vertical orientation

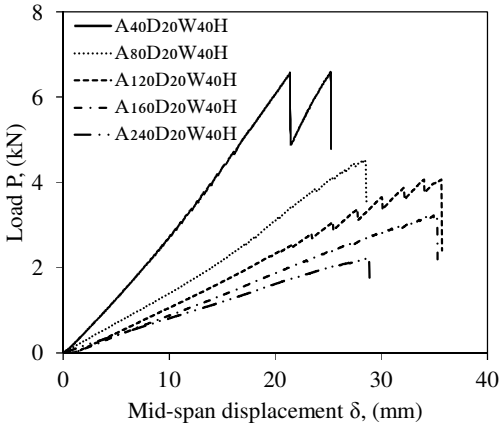

(c) 20 × 40 mm at horizontal orientation

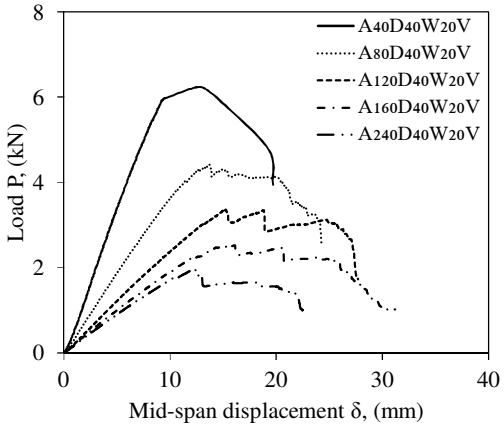

(d) 20 × 40 mm at vertical orientation

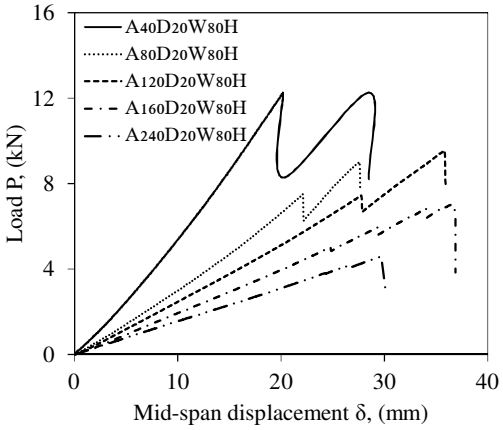

(e) 20 × 80 mm at horizontal orientation

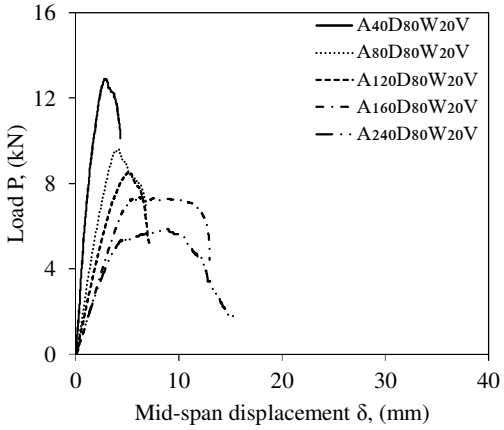

(f) 20 × 80 mm at vertical orientation

Fig. 3: Load-displacement behaviour of sandwich beams

ACCEPTED MANUSCRIPT

3.3. Bending and shear stiffness

The bending and shear stiffness of the beams were determined using the simultaneous method [22]. Bank [23] indicated that the total deflection of composite structures is the sum of the deflection due to bending and shear deformations. This applies to the composite sandwich beams due to the relatively low shear stiffness of the core compared to the GFRP skins. As a result, each of the sandwich beams tested in this study exhibited a load-displacement behaviour with two unknowns, EI and kGA as presented in Eq. (2) with $(3L^2 - 4a^2/48)$ being the independent variable while (δ/Pa) being the dependent variable. Figures 4(a) and 4(b) depict the graphical presentation of Eq. (2) for horizontal and vertical orientations with different beam dimensions and shear spans. The bending stiffness (EI) and shear stiffness (kGA) is determined from the slope and intercept of the fitted line, respectively.

$$\frac{\delta}{Pa} = \frac{1}{EI}\left(\frac{3L^2-4a^2}{48}\right) + \frac{1}{2kGA} \qquad (2)$$

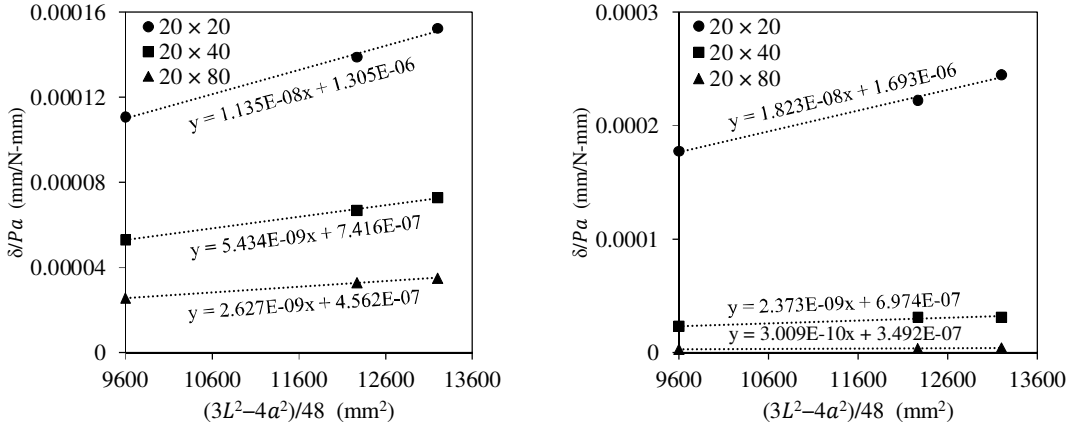

(a) horizontal orientation (b) vertical orientation

Fig. 4: Graphical presentation for determining bending and shear stiffness

Figure 4 shows the variation of (δ/Pa) with respect to $(3L^2 - 4a^2/48)$ for shear spans of $L/2, L/3$ and $L/4$. The effective bending modulus (E_{eff}) and effective shear modulus (G_{eff}) are evaluated by dividing with the equivalent moment of inertia and area of a

ACCEPTED MANUSCRIPT

rectangular section assuming that the sandwich beams are made up of a homogeneous material. The shear correction factor $k = 1$ is considered and G and A are the shear modulus and cross sectional area, respectively. The effective elastic properties of the sandwich beams are tabulated in Table 3.

Table 3: Stiffness properties of sandwich beams

Orientation	Beam section	EI (MPa-mm^4)	kGA (MPa-mm^2)	E_{eff} (GPa)	G_{eff} (GPa)
Horizontal	20 × 20	88×10^6	383×10^3	6.61	0.96
	20 × 40	184×10^6	674×10^3	6.90	0.84
	20 × 80	381×10^6	1096×10^3	7.14	0.69
			Horizontal average =	*6.88*	*0.83*
Vertical	20 × 20	55×10^6	295×10^3	4.11	0.74
	20 × 40	421×10^6	717×10^3	3.95	0.90
	20 × 80	3323×10^6	1432×10^3	3.89	0.89
			Vertical average =	*3.98*	*0.84*

In the horizontal orientation, Table 3 shows that the magnitude of EI and kGA are increasing almost proportionally with the increase of beam dimension. On the other hand, in vertical orientation, the increase of beam dimension exponentially increase the EI but proportionally increase the kGA. The average magnitude of E_{eff} is higher in horizontal orientation (6.88 GPa) than the vertical position (3.98 GPa). This is due to the separation of skins with respect to major axis of bending which contributed in improving the bending modulus of the beam at horizontal orientation but the separation does not contribute at vertical orientation. However, the magnitude of G_{eff} are similar regardless of beam orientation due to the equal area of the beam resisting the shear deformation.

ACCEPTED MANUSCRIPT

3.4. Effect of beam orientation

The change of beam orientation from horizontal to vertical changes the mode of failure of the sandwich beams. The sandwich specimens failed in brittle manner at horizontal orientation while the failure is progressive at vertical orientation. The load-displacement behaviour in Figure 3 has shown a sudden drop of load in horizontal orientation indicating a brittle nature of failure. The brittle failure occurred due to the core shear when specimen fails in shear, and combined shear and bending whereas this happened at bending failure due to core compression. On the other side, the gradual decline of load with the increase of displacement demonstrated the progressive failure of the skins due to shear, compression and tension. This failure behaviour indicates that the structure constructed with vertical sandwich beams will provide sufficient warning before the ultimate failure which is an important characteristics in civil engineering design. However, the load carrying behaviour in horizontal and vertical orientation depends on the sectional dimension of the beam. At a particular shear span, Figure 5 shows that the horizontal orientation carried higher loads than the vertical orientation for 20 mm × 20 mm and 20 mm × 40 mm beams whereas the vertical orientation carried greater magnitude of loads than the horizontal position for 20 mm × 80 mm sectional beam. This is due to the effective utilisation of skin's strength at horizontal orientation for 20 mm × 20 mm and 20 mm × 40 mm section where separation of skins with respect to the major axis of bending are more effective in carrying loads than the vertical orientation of skins. On the other hand, the effect of skin depth in vertical orientation become more effective than the skin separation in horizontal orientation for 20 mm × 80 mm section. The gradual increase of beam dimension exponentially increase the load carrying capacity at vertical orientation while the increase of load capacity is only linear at horizontal orientation with the increase of beam dimension. Glenn and Francis [24] indicated that the load-carrying capacity of a beam can greatly increase by its depth. Moreover, the increase of depth increased the shear

ACCEPTED MANUSCRIPT

dominance on the vertical beams and the higher load carrying capacity of the vertical beams at larger section (20 mm × 80 mm) indicating the vertical orientation is preferable against shear. Figure 5 shows that, for any shear span, the horizontal and vertical curves intersects in the range between 50 mm and 60 mm. Results indicated that the transitional sectional dimension is between 50 mm and 60 mm with an average of 55 mm, below which the horizontal and above which the vertical orientation can carry higher load.

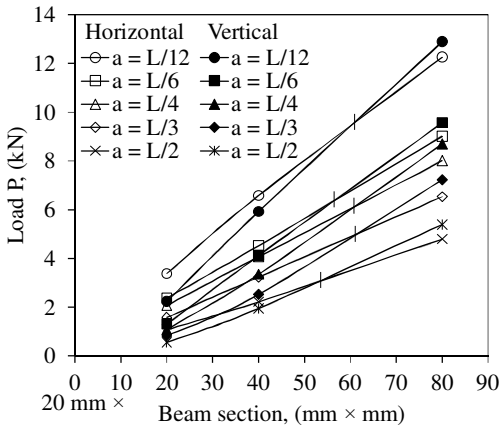

Fig. 5: Load carrying capacity at horizontal and vertical orientation

Table 3 shows that the bending stiffness of sandwich beam is greatly influenced by the orientation. For 20 mm × 20 mm beam, the bending stiffness of beams at the vertical orientation is only 63% of beams at the horizontal orientation. This is expected for the square cross sectional beam where the separation of skins contributed more to the bending stiffness at horizontal orientation than the vertical position. The bending stiffness at vertical orientation increased 2.29 and 8.73 times than the horizontal orientation for 20 mm × 40 mm and 20 mm × 80 mm beams, respectively. This result suggests that the larger the sectional dimension, the sandwich beams are more effective when positioned vertically than horizontally to minimise the amount of total deflection. This efficiency is due to the increase of skin depth at vertical orientation which significantly contributed to the increase of bending stiffness. For any sectional dimension, the contribution of core is 8% and 23% for horizontal

ACCEPTED MANUSCRIPT

and vertical orientations respectively, indicating both core and skin significantly contributed to the bending stiffness at vertical orientation. Therefore, the bending stiffness of the sandwich beam with fibre composite skins and high strength core primarily depends on the modulus of elasticity, sectional dimension and orientation of the constituent materials. Chakrabortty et al. [25] indicated the low stiffness of fibre composite structure is a great concern and can only be addressed through innovative design. Thus, the high bending stiffness of the sandwich structure can be efficiently utilised by placing the beams at vertical orientation, particularly when the depth-to-width ratio is 2 or more (e.g., 20 mm × 40 mm and 20 mm × 80 mm beam).

3.5. Effect of shear span-to-depth ratio

The variation of failure mode of the specimens at horizontal and vertical orientation with different shear span-to-depth (a/d) ratios are plotted in Figures 6(a) and 6(b), respectively. These figures suggested that a/d ratio has strong influence on the failure mode of the sandwich beams. Generally, the beams failed in shear when a/d $\leq$ 2, specifically, the horizontal beams failed in core shear (Fig. 2a) and vertical beams failed by skin shear (Fig. 2b). However, an exception was observed in 80 mm depth beam at vertical orientation which failed by indentation due to the high local compression (Fig. 2g). With the increase of a/d ratio, the shear dominance on the beam decreases and the bending effect increases. The sandwich beams failed due to the combined effect of shear and bending for 2 < a/d < 6. Within this a/d range, the horizontal specimens failed in core shear followed by debonding between the core and the top skin due to the effect of bending (Fig. 2c). In vertical orientation, the diagonal cracks in vertical skins arose from shear effect, and the compressive and tensile failure of the skins were developed due to the bending effect (Fig. 2d and 2h). From an experimental investigation of the sandwich beams at horizontal orientation, Manalo [18] observed a transitional zone for a/d ratios between 3 and 6, where the specimens

ACCEPTED MANUSCRIPT

experienced both shear and bending. In the present study when a/d ≥ 6, the bending failure was observed for the specimens. The bending failure of horizontal beams was confirmed with the skin compression followed by core compression and debonding (Fig. 2e). The buckling of the skins due to compression, and tensile fracture of the skins are the indication of bending failure in vertical orientation for a/d ≥ 6 (Fig. 2f). In contrast, Mathieson and Fam [19] observed the buckling failure of the skin at a/d ratios between 1.33 and 4.67 for soft core sandwich beam. This suggests the better stability of the vertical skins due to the high strength phenolic core compared to the soft core material which can provide only a low tensile bond strength between the core and the skin.

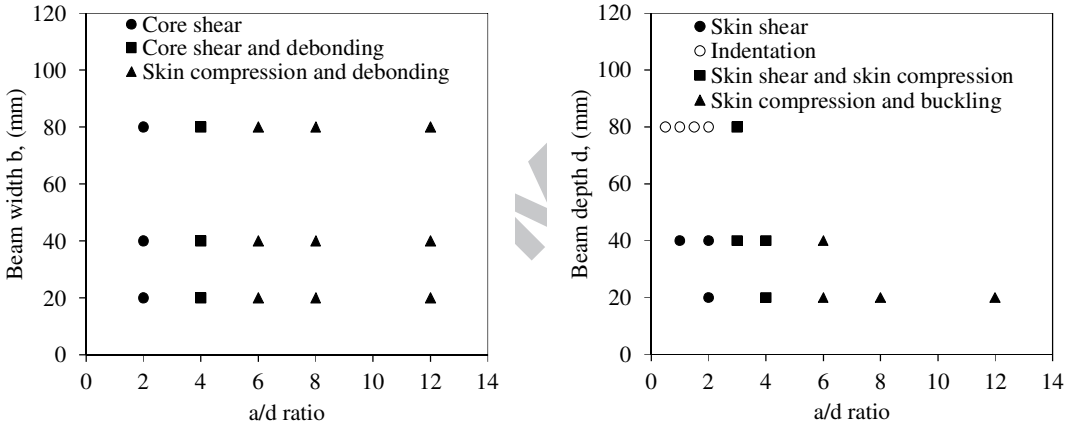

(a) horizontal orientation (b) vertical orientation

Fig. 6: Failure of the beam at different shear span-to-depth ratios

The bending stress of the extreme fibres in both horizontal and vertical orientations can be calculated by Eq. (3).

$$\sigma_s = \frac{M(d/2)}{EI} E_s \quad (3)$$

where, σ_s, M, d, E_s, and EI represent the bending stress of the skin, bending moment at failure load, depth of the beam, elastic modulus of the skin, and bending stiffness (Table 3) of the beam, respectively. When the average shear stress in the core is determined, the skin is transformed into an equivalent core using the shear modular ratio. On the other hand, the core

ACCEPTED MANUSCRIPT

was transformed into an equivalent skin area if the average shear stress is determined for skin [14]. The average shear stress in core (τ_c) at horizontal orientation and the average shear stress in skin (τ_s) at vertical orientation are calculated using Eq. (4) and Eq. (5), respectively. Where, G_c and G_s represents the shear modulus of core and skin respectively.

$$\tau_c = \frac{(P/2)}{[t_c+2t_s(G_s/G_c)]b} \quad (4)$$

$$\tau_s = \frac{(P/2)}{[2t_s+t_c(G_c/G_s)]d} \quad (5)$$

The variation of bending and shear stress with respect to the a/d ratio for both horizontal and vertical orientations are shown in Figure 7. The bending stress increases with the increase of a/d ratio from 2 to 6 and gradually become constant when a/d > 6. This is due to the similar mode of failure for all specimens at horizontal (i.e., skin compression and debonding) or vertical orientations (i.e., skin compression and buckling) when a/d > 6 as shown in Figure 6(a) and 6(b). From Figure 7(a), it can be seen that the bending stress at horizontal orientation is higher than the vertical position when the beam fails in bending. The maximum compressive bending stress in the skin was 237 MPa at horizontal orientation which is close to the average compressive strength of skin determined from the test of coupons as reported in Table 1. However, the vertical beams failed only at 220 MPa compressive bending stress. This can be attributed to the failure mode of the vertical beams due to a combined skin compression and buckling. The buckling failure is exhibited in the form of debonding of the skins from the core as shown in Figure 2(f). Mathieson and Fam [19] observed that the buckling of skin in the sandwich beam arises before the skin reaches to its ultimate compressive strength due to the low tensile bond between the core and the skins. This explains why the beams in vertical orientation failed at lower bending stress for a/d ≥ 6 and indicating the preference of horizontal orientation for the design of bending dominated structures. It is important to note that the load at which buckling failure of the vertical skins occurred was almost 92% of the maximum compressive stress of the fibre composites. In

ACCEPTED MANUSCRIPT

contrast, the buckling of the skin for sandwich beams with a soft core investigated by Mathieson and Fam [19] is only at 50%. This result further suggest the suitability of a phenolic core in providing stability to the vertical skins.

Figure 7(b) shows that the shear stress decreases with the increase of a/d ratio. Dai and Hahn [26] and Awad et al. [27] indicated that the sandwich beams with shorter shear span exhibited higher shear stress than the longer shear span. However, there is a clear distinction of shear stress level between horizontal and vertical orientations (Fig. 7b). At horizontal orientation, the core is mainly carrying the shear force whereas the shear force is carried by both the core and the skins at vertical orientation. As a result, for the same a/d ratio, the shear stress at failure is significantly higher at vertical orientation than the horizontal position. This indicates that the sandwich structure is more effective in carrying shear if they are to be applied in the vertical orientation.

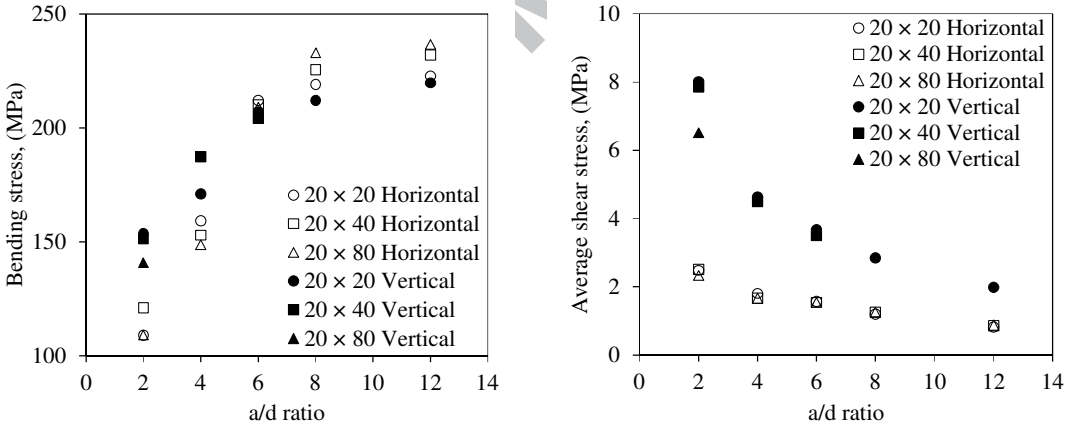

(a) variation of bending stress with a/d ratio (b) variation of shear stress with a/d ratio

Fig. 7: Effect of a/d ratio on bending and shear stress at different orientations

Manalo [18] indicated that the different failure modes observed for the sandwich beams with different a/d ratios can be explained by the shear-to-bending stress ratio. Thus, the variation of shear-to-bending stress (τ/σ) with a/d ratio at horizontal and vertical orientations are plotted in Figures 8(a) and 8(b), respectively. Based on the failure

ACCEPTED MANUSCRIPT

mechanism, in horizontal orientation the τ/σ ratio was calculated as the ratio of the actual shear stress in the core and the bending stress of the skin while this ratio was determined as the actual shear and bending stress of the skin at vertical orientation. Figure 8 shows that the τ/σ ratio decreases due to the decrease of shear effect and increase of bending influence with the increase of a/d ratio. Yoshihara and Furushima [28] indicated that when the actual τ/σ ratio is larger than the allowable τ/σ ratio, the timber specimen would fail in shear. In horizontal orientation, the upper bound allowable stress ratio (0.014) is calculated as the ratio of shear strength of core to the tensile strength of skin while the lower bound (0.009) is the ratio of shear strength of core to the bending strength of skin. Similarly, in vertical orientation, the upper bound allowable stress ratio (0.079) is calculated as the ratio of shear strength of skin to the tensile strength of skin while the lower bound (0.051) is the ratio of shear strength of skin to the bending strength of skin. This is due to the core shear failure at horizontal orientation and skin shear failure at vertical orientation as mentioned earlier. During shear failure, the actual bending stress in the skin is lower than the skins' maximum bending strength and thus the tensile strength of skin is considered for determining the upper bound stress ratio. The upper and lower bound allowable stress ratio is particularly important in determining the zone of shear and bending failure. When the actual τ/σ ratio is higher than the upper bound allowable τ/σ ratio, the sandwich beams are expected to fail in shear. On the other hand, the sandwich specimens are expected to fail in bending if the actual τ/σ ratio is lower than the lower bound allowable τ/σ ratio. Moreover, if the actual τ/σ ratio falls between the upper and lower bound allowable limit, the sandwich beams are expected to fail in combined shear and bending. Figure 8(a) shows that the stress ratio concept can accurately predict the mode of failure of the sandwich beams at horizontal orientation. However, at vertical orientation, the upper and lower bound allowable stress ratio is slightly higher than the expectation. This may be attributed to the progressive nature of failure of the beams at

ACCEPTED MANUSCRIPT

vertical orientation which provided several load drops at different displacements. This result also indicate that the vertical beams are superior in shear performance and prediction of failure behaviour is more complex than the horizontal orientation.

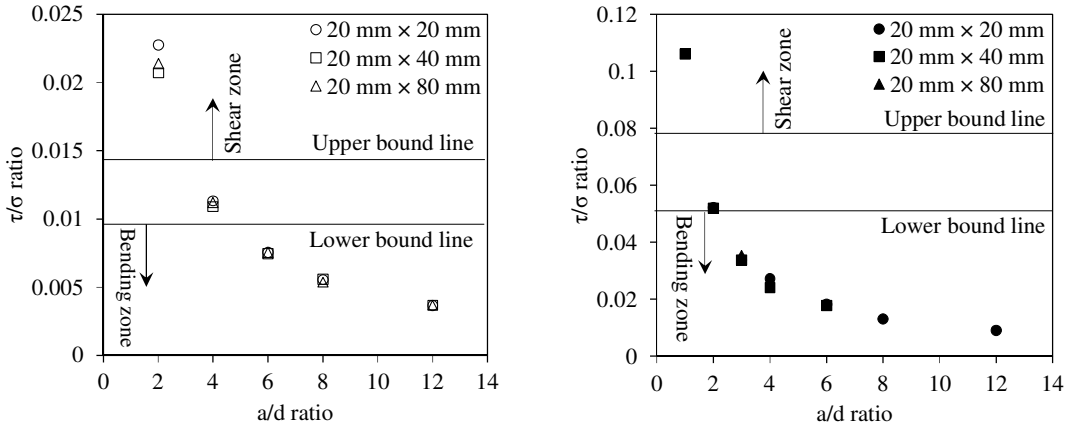

(a) specimens at horizontal orientation (b) specimens at vertical orientation

Fig. 8: Effect of a/d ratio on shear-to-bending stress ratio

3.6. Determination of the influence of the variables

The influence of beam orientation and a/d ratio on the load carrying capacity and stiffness properties of the sandwich beam was evaluated by a two-way Analysis of Variance (ANOVA) using SPSS - a statistical analysis software [29]. As it is mentioned, the change of failure modes from shear to bending occur when a/d ratio changes from 2 to 6 in both horizontal and vertical orientations, therefore, the variation of a/d is considered in that range for this analysis. The results of two-way ANOVA are shown in Table 4.

Table 4: Two-way ANOVA results

Dependent variable	Independent variable	F-value	p-value	Partial eta squared (η_p^2)
Failure loads	Orientation	3.941	0.075	0.283
	a/d ratio	1.333	0.307	0.210
Bending stiffness	Orientation	3.066	0.105	0.203
	a/d ratio	0.000	1.000	0.000

ACCEPTED MANUSCRIPT

Table 4 indicates that the variation of failure loads and bending stiffness for different test setup are not statistically significant ($p > \alpha$) with 95% confidence interval ($\alpha = 0.05$) due to the change of orientation and a/d ratio. However, the influence of orientation and a/d ratio on the failure loads and bending stiffness are not same which is represented by η_p^2. The result of the analysis shows that 28.3% of the variability of failure loads is being accounted by orientation while a/d ratio is responsible for 21% variation. On the other hand, 20.3% of the variability of bending stiffness is being accounted by orientation while a/d ratio has no influence on the bending stiffness. This concludes that the orientation of the sandwich beam is a more influential parameter than the a/d ratio. The distance between the skins at horizontal orientation plays significant role on load carrying capacity while the separation of skins at vertical orientation does not have significant effect that makes the beam orientation an influential parameter. Moreover, the bending stiffness of the beam affected by its orientation but does not depends on the loading position.

4. Theoretical Analysis

4.1. Estimation of failure loads

This section discussed the theoretical estimation of failure loads for different configuration of sandwich beams. The experimentally observed failure modes, i.e. bending failure, shear failure, combined shear and bending failure, and indentation failure were considered as the criterion to estimate the load capacity of the sandwich beams.

4.1.1. Bending failure

The sandwich beam is expected to fail in bending when the bending stress of the skin (σ_s) reaches to the allowable compressive bending stress of the skin ($\sigma_{s(all)}$). Simplifying Eq. (3), the ultimate failure load due to bending (P_b) of sandwich beams with horizontal and vertical orientations can be determined by Eq. (6).

ACCEPTED MANUSCRIPT

$$P_b = \frac{4(EI)\sigma_{s(all)}}{adE_s} \quad (6)$$

The theoretical bending stiffness EI in horizontal and vertical orientations can be calculated by Eq. (7) and Eq. (8), respectively.

In horizontal orientation,

$$EI = \frac{bt_c^3}{12}E_c + \frac{bt_s}{2}\left(\frac{t_s^2}{3} + {d_0}^2\right)E_s \quad (7)$$

In vertical orientation,

$$EI = \frac{t_c d^3}{12}E_c + \frac{t_s d^3}{6}E_s \quad (8)$$

4.1.2. Shear failure

The shear stress at different levels of the sandwich beam section can be determined by accounting the constituent materials of the cross section [30]. In horizontal orientation, the sandwich beam is expected to fail in shear when the shear stress of the phenolic core reaches its allowable shear strength ($\tau_{c(all)}$). In vertical position, shear failure occurs when the shear stress in the skin exceeds the allowable shear strength of the skin ($\tau_{s(all)}$) [14]. The shear failure load (P_s) in horizontal and vertical orientations of the beam can be determined by Eq. (9) and Eq. (10), respectively [14].

In horizontal orientation,

$$P_s = \frac{16(EI)\tau_{c(all)}}{4E_s t_s d_0 + E_c t_c^2} \quad (9)$$

In vertical orientation,

$$P_s = \frac{4d\tau_{s(all)}}{3}\left(2t_s + t_c\frac{E_c}{E_s}\right) \quad (10)$$

The bending stiffness EI in Eq. (9) can be calculated by Eq. (7).

4.1.3. Combined shear and bending failure

When shear span-to-depth ratios are between 2 and 6, the failure of the sandwich beam occurs due to the combined action of shear and bending. Bank [23] indicated that, when a

ACCEPTED MANUSCRIPT

beam is subjected to high shear forces and high bending moment, a combined shear and bending action will govern. Under this circumstances, the maximum stress criterion can be used in predicting failure loads. The failure is expected when the sum of the ratios of actual shear stress (τ_{act}) to allowable shear stress (τ_{all}) and actual bending stress (σ_{act}) to allowable bending stress (σ_{all}) approaches unity. The linear failure criterion can be expressed as:

$$\frac{\tau_{act}}{\tau_{all}} + \frac{\sigma_{act}}{\sigma_{all}} = 1 \tag{11}$$

Simplifying Eq. (11) using Eqs. (6 to 10), the failure loads can be calculated as:

In horizontal orientation,

$$P_{s-b} = \frac{1}{\left[\frac{4E_S t_S d_0 + E_C t_C^2}{16(EI)\tau_{c(all)}} + \frac{adE_S}{4(EI)\sigma_{s(all)}}\right]} \tag{12}$$

In vertical orientation,

$$P_{s-b} = \frac{1}{\left[\frac{3E_S}{4d(2t_S E_S + t_C E_C)\tau_{s(all)}} + \frac{adE_S}{4(EI)\sigma_{s(all)}}\right]} \tag{13}$$

In Eq. (12) and Eq. (13), P_{s-b} is the failure load due to combined action of shear and bending. $\tau_{c(all)}$ and $\tau_{s(all)}$ are the allowable shear stress in core and skin, respectively and $\sigma_{s(all)}$ is the allowable compressive stress of skin. The bending stiffness in horizontal and vertical orientations can be determined by Eq. (7) and Eq. (8), respectively.

4.1.4. Indentation failure

The theoretical model for predicting indentation failure loads of foam-core sandwich beams at horizontal orientation have been studied by several researchers [31-35]. However, there is a lack of research for estimating indentation failure loads at vertical orientation. The present study proposed a theoretical model for estimating indentation failure loads at vertical orientation based on the principle of contact mechanics theory [36]. Two assumptions have been considered for indentation modelling; (a) the beam is supported on rigid plastic foundation [31], and (b) the indentation failure occurs when the stress in skins under the

ACCEPTED MANUSCRIPT

indenter attains to the transverse compressive strength of the skin. The mechanism of transferring loads from the indenter to the sandwich beam through a line contact at the early stage of load application and the contact area increase with the increase of applied loads as shown in Figure 9.

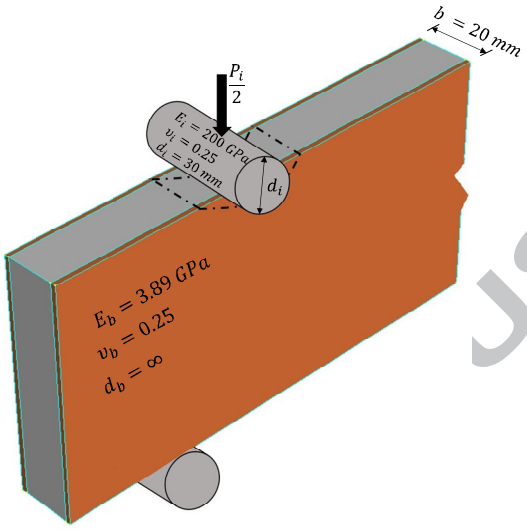

Fig. 9: Indentation failure modelling using contact mechanics theory

According to contact theory, when indentation occurs, the half width of the contact zone can be expressed by Eq. (14).

$$b_h = K_b\sqrt{\frac{P_i}{2}} \tag{14}$$

In Eq. (14), b_h and P_i represents the half width of the contact zone and the applied load at which indentation failure occurs, respectively. The other parameter K_b can be expressed by Eq. (15).

$$K_b = \sqrt{\frac{2}{\pi b}\frac{\left(\frac{1-\nu_i^2}{E_i}+\frac{1-\nu_b^2}{E_b}\right)}{\left(\frac{1}{d_i}+\frac{1}{d_b}\right)}} \tag{15}$$

In Eq. (15), b is the beam width (contact length), ν_i, E_i and d_i are the poisson's ratio, elastic modulus and diameter of the indenter, respectively. Similarly, ν_b, E_b and d_b are the poisson's ratio, elastic modulus and diameter of the sandwich beam, respectively. The effective elastic

ACCEPTED MANUSCRIPT

modulus of the 20 mm × 80 mm beam at vertical orientation is determined in Table 3. As the contact zone of the sandwich beam is a plane surface, the diameter of the beam is considered infinite. The indentation failure loads, P_i can be determined by Eq. (16).

$$P_i = (\pi b_h b)\sigma_{tcs} \quad (16)$$

In Eq. (16), σ_{tcs} is the transverse compressive strength of the skin as provided in Table 1.

4.1.5. Comparison between calculated and actual failure load

The calculated failure loads from the appropriate theoretical model presented in Eq. (6), Eq. (9), Eq. (10), Eq. (12), Eq. (13) and Eq. (16) are provided in Table 2 and compared it with the actual failure loads of the beam. Shear based equation (Eq. 9 and Eq. 10) can reliably predict the failure load for a/d ratio up to 2. On the other hand, bending equation (Eq. 6) can estimate the failure loads when a/d ratio is equal to or greater than 6. However, when a/d ratio is between 2 and 6, the combined shear and bending equations (Eq. 12 and Eq. 13) are the most reliable. The indentation failure model in Eq. (16) can reliably estimate the failure loads for 80 mm deep vertical sandwich beams with a/d ratio of 2. The loads calculated from Eq. (16) represents the initiation of the indentation, and with the gradual decrease of a/d ratio the effect of shear compression increase and the ultimate failure occurs at higher loads even the early initiation of indentation (Fig. 2g). However, a combined shear and bending failure was observed for a/d of 3 and Eq. 13 provided a reliable estimation.

From the percentage differences (% Diff.) between experimental and theoretical failure loads in Table 2, it can be seen that the theoretical model mostly underestimates the ultimate load when the sandwich beam fails in shear. On the other hand, the bending failure equation overestimates the failure load due to the initiation of debonding between the skin and the core. It is important to note that in the considered theoretical analyses, the skin is assumed perfectly bonded to the core. This separation from the core resulted in the thin fibre composite to buckle in both beam orientation. In most cases, the traditional theoretical

ACCEPTED MANUSCRIPT

models estimated the shear failure loads within 30%, combined shear and bending failure loads within 25%, and bending failure loads within 20% of the experimental failure loads. This indicates the classical failure models can estimate the bending failure loads more reliably than the shear failure loads. Moreover, the greater variation between predicted and actual failure loads was obtained at vertical orientation than the horizontal position. This is due to the more complex behaviour of vertical beams than the horizontal one as explained in Fig. 8. The proposed indentation failure model for vertical orientation satisfactorily measures the initiation of the indentation failure loads. However, this model cannot describe how the shear span affected the load carrying capacity which seems an important effect during indentation. The high actual indentation load compared to the predicted value for vertical beams with a/d < 2 is due to the effect of shear compression which have allowed the beam to continuously carry the load. This failure mechanism needs further investigation. In many circumstances, researchers have found the differences between experimental and theoretical failure loads of sandwich beams up to 20% [19], 21% [31], 30% [37], 34% [18], and even up to 100% [7]. Therefore, further investigation is necessary to establish better theoretical models that can capture the insight into the response of the sandwich beams.

4.2. Theoretical evaluation of bending and shear stiffness

Experimentally, the bending stiffness (EI) and shear stiffness (kGA) are evaluated from the load-displacement relationship and presented in Table 3. Theoretically, the bending stiffness of sandwich beams in horizontal and vertical orientations can be estimated using Eq. (7) and Eq. (8), respectively, by assuming the skins and core are perfectly bonded [38]. However, for a particular sandwich beam, theoretically the shear stiffness in horizontal and vertical orientations can be estimated by Eq. (17).

$$kGA = k[G_s A_s + G_c A_c] \quad (17)$$

ACCEPTED MANUSCRIPT

Where, G_s, A_s, G_c and A_c are the shear modulus and cross sectional area of skins and core for the beam section, and the shear correction factor $k = 1$ as mentioned earlier. A comparison between the experimental and theoretical stiffness are depicted in Figure 10. Results shows that the analytical equations can satisfactorily estimate the actual bending stiffness of the sandwich beams.

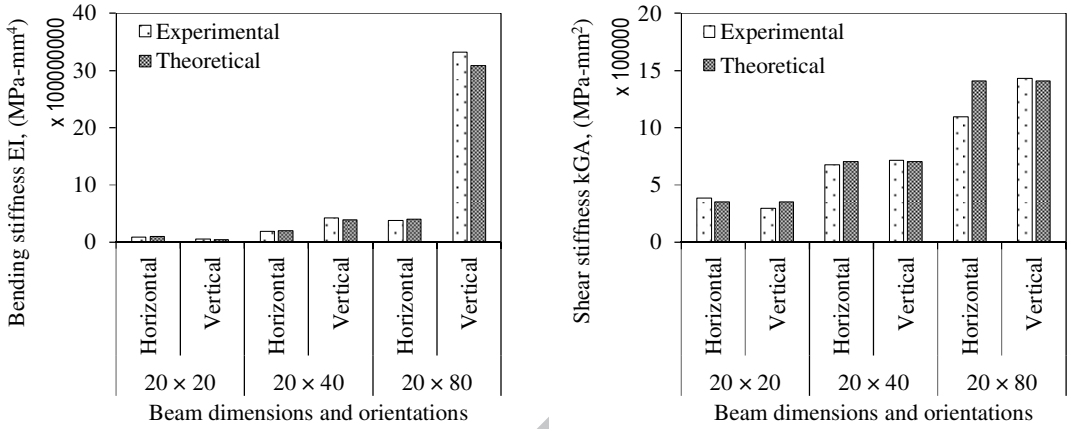

(a) bending stiffness (b) shear stiffness

Fig. 10: Comparison between experimental and theoretical stiffness

5. Conclusions

A series of experimental tests were carried out on 30 specimens to evaluate the properties and to understand the flexural and shear behaviour of phenolic core sandwich beams at different orientations. The load-displacement behaviour, failure mode, strength and stiffness of beams were systematically investigated. The findings of the present study can be summarised as follows:

- The sandwich beam fails in brittle manner at horizontal orientation while the failure is progressive at vertical orientation. With the increase of sectional dimension but same shear span, the sandwich beam fails in similar mode at horizontal orientation but fails differently at vertical orientation.

ACCEPTED MANUSCRIPT

- The transitional sectional dimension of the beam is approximately 20 mm × 55 mm, below which the horizontal orientation and above which the vertical orientation carried higher loads.
- The bending stiffness of the sandwich beam is greatly influenced by its orientation and can be efficiently utilised by placing the beams vertically, particularly when the beam depth-to-width ratio is 2 or more.
- Generally, the sandwich beam fails in shear, a combined shear and bending, and bending for shear span-to-depth ratios of 2 or less, between 2 and 6, and 6 or more, respectively. The possibility of indentation failure is higher at vertical orientation than the horizontal position.
- Sandwich beams in the horizontal orientation is preferable for designing bending dominated structure while vertical orientation is a superior choice for shear dominated structure.
- The beams are expected to fail in shear when the actual shear-to-bending stress ratio is higher than the allowable shear-to-tensile stress ratio while the beams are more likely to fail in bending when the actual shear-to-bending stress ratio is lower than the allowable shear-to-bending stress ratio. In between these ratios, a combined shear and bending failure is expected.
- The two-way Analysis of Variance showed that the beam orientation has more influence on the load carrying capacity and stiffness properties than changing the shear span-to-depth ratio.
- The existing theoretical models can estimate more reliably the failure loads in bending than in shear. The proposed indentation failure model reliably estimated the initiation of indentation in the vertical orientation. These moderate variation of failure loads predicted by existing models suggested a further investigation to establish better

ACCEPTED MANUSCRIPT

theoretical models that can capture other critical behaviour such as the initiation of skin debonding and the shear compression failure of the very short vertical sandwich beams.

ACCEPTED MANUSCRIPT

ACCEPTED MANUSCRIPT

Acknowledgement

The first author gratefully acknowledged the financial support through Australian Postgraduate Award (APA) scholarship from the University of Southern Queensland, Australia for carrying out his PhD study. Authors are also grateful to Professor Gerard Van Erp for his valuable suggestions and acknowledged the materials support by the Department of Industry Innovation, Science, Research and Tertiary Teaching Enterprise Connect Researcher-In-Business Funded by the Australian Government.

References

[1] Manalo A, Aravinthan T, Fam A, Benmokrane B. State-of-the-art review on FRP sandwich systems for lightweight civil infrastructure. Journal of composites for construction. 2016.
[2] Keller T. Material-tailored use of FRP composites in bridge and building construction. CIAS International Seminar. Cyprus2007.
[3] Van Erp G, Rogers D. A highly sustainable fibre composite building panel. Sustainable Procurement Conference. Brisbane, Australia2008.
[4] Tomlinson D, Fam A. Flexural behavior of precast concrete sandwich wall panels with basalt FRP and steel reinforcement. PCI journal. 2015:51-71.
[5] Manalo AC, Aravinthan T. Behaviour of full-scale railway turnout sleepers from glue-laminated fibre composite sandwich structures. Journal of composites for construction. 2012;16:724-36.
[6] Ferdous W, Manalo A, Van Erp G, Aravinthan T, Kaewunruen S, Remennikov A. Composite railway sleepers – Recent developments, challenges and future prospects. Composite Structures. 2015;134:158–68.
[7] Russo A, Zuccarello B. Experimental and numerical evaluation of the mechanical behaviour of GFRP sandwich panels. Composite Structures. 2007;81:575–86.
[8] Kashtalyan M, Menshykova M. Three-dimensional elasticity solution for sandwich panels with a functionally graded core. Composite Structures. 2009;87:36–43.
[9] Styles M, Compston P, Kalyanasundaram S. The effect of core thickness on the flexural behaviour of aluminium foam sandwich structures. Composite Structures. 2007;80:532–8.
[10] Belouettar S, Abbadi A, Azari Z, Belouettar R, Freres P. Experimental investigation of static and fatigue behaviour of composites honeycomb materials using four point bending tests. Composite Structures. 2009;87:265–73.
[11] Deshpande VS, Fleck NA. Collapse of truss core sandwich beams in 3-point bending. International Journal of Solids and Structures. 2001;38:6275–305.
[12] Fam A, Sharaf T. Flexural performance of sandwich panels comprising polyurethane core and GFRP skins and ribs of various configurations. Composite Structures. 2010;92:2927–35.
[13] Mostafa A, Shankar K, Morozov EV. Behaviour of PU-foam/glass-fibre composite sandwich panels under flexural static load. Materials and Structures. 2014;48:1545–59.

ACCEPTED MANUSCRIPT

[14] Manalo AC, Aravinthan T, Karunasena W, Islam MM. Flexural behaviour of structural fibre composite sandwich beams in flatwise and edgewise positions. Composite Structures. 2010;92:984-95.
[15] El-Hacha R, Abdelazeem H, Cariaga I. Effect of casting method and shear span-to-depth ratio on the behaviour of Ultra-High Performance Concrete cross arms for high voltage transmission lines. Engineering Structures. 2010;32:2210–20.
[16] Kotsovos MD, Pavlović MN. Size effects in beams with small shear span-to-depth ratios. Computers & Structures. 2004;82:143–56.
[17] Danawade BA, Malagi RR, Kalamkar RR, Sarode AD. Effect of span-to-depth ratio on flexural properties of wood filled steel tubes. International Conference on Advances in Manufacturing and Materials Engineering: Procedia Materials Science, Elsevier; 2014. p. 96-105.
[18] Manalo AC. Behaviour of fibre composite sandwich structures under short and asymmetrical beam shear tests. Composite Structures. 2013;99:339–49.
[19] Mathieson H, Fam A. In-plane bending and failure mechanism of sandwich beams with GFRP skins and soft polyurethane foam core. Journal of composites for construction. 2016;20:1-10.
[20] Bootle KR. Wood in Australia: Types, properties and uses: McGraw-Hill, 2005.
[21] ASTM-C393. ASTM Standard: Standard test method for core shear properties of sandwich constructions by beam flexure. 2016.
[22] Muttashar M, Karunasena W, Manalo A, Lokuge W. Behaviour of hollow pultruded GFRP square beams with different shear span-to-depth ratios. Journal of Composite Materials. 2015:1-16.
[23] Bank LC. Composites for construction : structural design with FRP materials. New Jersey: John Wiley & Sons, Inc, 2006.
[24] Corbett GP, Brannigan FL. Brannigan's Building Construction for the Fire Service. 5th ed: Jones & Bartlett, 2013.
[25] Chakrabortty A, Khennane A, Kayali O, Morozov E. Performance of outside filament-wound hybrid FRP-concrete beams. Composites Part B: Engineering. 2011;42:907–15.
[26] Dai J, Hahn HT. Flexural behavior of sandwich beams fabricated by vacuum-assisted resin transfer molding. Composite Structures. 2003;61:247–53.
[27] Awad ZK, Aravinthan T, Manalo A. Geometry effect on the behaviour of single and glue-laminated glass fibre reinforced polymer composite sandwich beams loaded in four-point bending. Materials & Design. 2012;39:93–103.
[28] Yoshihara H, Furushima T. Shear strengths of wood measured by various short beam shear test methods. Wood Science and Technology. 2003;37:189-97.
[29] Nie NH. SPSS : statistical package for the social sciences. New York: McGraw-Hill, 1975.
[30] Triantafillou TC. Composites: a new possibility for the shear strengthening of concrete, masonry and wood. Composites Science and Technology. 1998;58:1285–95.
[31] Gdoutos EE, Daniel IM, Wang KA. Indentation failure in composite sandwich structures. Experimental mechanics. 2002;42:426–31.
[32] Xie Z-Y, Yu J-L, Zheng Z-J. A plastic indentation model for sandwich beams with metallic foam cores. Acta Mechanica Sinica. 2011;27:963–6.
[33] Li Z, Chen X, Jiang B, Lu F. Local indentation of aluminum foam core sandwich beams at elevated temperatures. Composite Structures. 2016;145:142–8.
[34] Petras A, Sutcliffe MPF. Indentation failure analysis of sandwich beams. Composite Structures. 2000;50:311–8.

ACCEPTED MANUSCRIPT

[35] Galletti GG, Vinquist C, Es-Said OS. Theoretical design and analysis of a honeycomb panel sandwich structure loaded in pure bending. Engineering Failure Analysis. 2008;15:555–62.
[36] Collins JA, Busby HR, Staab GH. Mechanical design of machine elements and machines: A failure prevention perspective: John Wiley & Sons, 2010.
[37] Mostafa A, Shankar K, Morozov EV. Experimental, theoretical and numerical investigation of the flexural behaviour of the composite sandwich panels with PVC foam core. Applied Composite Materials. 2014;21:661–75.
[38] Steeves CA, Fleck NA. Collapse mechanisms of sandwich beams with composite faces and a foam core, loaded in three-point bending. Part I: analytical models and minimum weight design. International Journal of Mechanical Sciences. 2004;46:561–83.

ACCEPTED MANUSCRIPT